AGU PUBLICATIONS

Geophysical Research Letters

RESEARCH LETTER
10.1002/2015GL063296

Key Points:
- CryoSat-2 radar altimetry was applied to 2012 Greenland melt event
- Surface melt introduces an elevation bias by changing snow scattering properties
- In situ observations confirm a significant bias in retrieved surface height

Supporting Information:
- Texts S1-S7 and Figures S1 and S2
- Figure S1
- Figure S2

Correspondence to:
J. Nilsson,
jnils@space.dtu.dk

Citation:
Nilsson, J., et al. (2015), Greenland 2012 melt event effects on CryoSat-2 radar altimetry, *Geophys. Res. Lett.*, *42*, 3919–3926, doi:10.1002/2015GL063296.

Received 30 JAN 2015
Accepted 15 APR 2015
Accepted article online 22 APR 2015
Published online 19 MAY 2015

Greenland 2012 melt event effects on CryoSat-2 radar altimetry

Johan Nilsson[1], Paul Vallelonga[2], Sebastian B. Simonsen[1], Louise Sandberg Sørensen[1], René Forsberg[1], Dorthe Dahl-Jensen[2], Motohiro Hirabayashi[3], Kumiko Goto-Azuma[3], Christine S. Hvidberg[2], Helle A. Kjær[2], and Kazuhide Satow[4]

[1]DTU Space, National Space Institute Technical University of Denmark, Lyngby, Denmark, [2]Centre for Ice and Climate, Niels Bohr Institute, University of Copenhagen, Copenhagen, Denmark, [3]National Institute of Polar Research, Tachikawa, Japan, [4]Nagaoka National College of Technology, Nagaoka, Japan

Abstract CryoSat-2 data are used to study elevation changes over an area in the interior part of the Greenland Ice Sheet during the extreme melt event in July 2012. The penetration of the radar signal into dry snow depends heavily on the snow stratigraphy, and the rapid formation of refrozen ice layers can bias the surface elevations obtained from radar altimetry. We investigate the change in CryoSat-2 waveforms and elevation estimates over the melt event and interpret the findings by comparing in situ surface and snow pit observations from the North Greenland Eemian Ice Drilling Project camp. The investigation shows a major transition of scattering properties around the area, and an apparent elevation increase of 56 ± 26 cm is observed in reprocessed CryoSat-2 data. We suggest that this jump in elevation can be explained by the formation of a refrozen melt layer that raised the reflective surface, introducing a positive elevation bias.

1. Introduction

The European Space Agency (ESA) CryoSat-2 satellite was launched in late 2010 and carries a new type of radar altimeter especially designed for monitoring the changes of sea and land ice. The radar altimeter transmits and receives a microwave signal reflected from the Earth's surface, commonly referred to as a waveform, which is used to determine the surface height using a procedure called retracking. The shape of the radar waveform is evaluated, as a function of delay time and contains important information about the characteristics of the measured surface. Radar waveform changes makes it possible to identify sudden and abrupt changes of the surface conditions of the ice sheet, such as snow melt or heavy snowfall [*Legresy and Rémy*, 1997].

In the interior parts of the Greenland Ice Sheet, the majority of the surface is dry snow (defined as snow that has not been subjected to liquid water). This snow is slowly transformed to ice within the top 50–100 m of the ice sheet, commonly referred to as the firn column. The dielectric properties of the firn vary throughout the column and also differ substantially from those of solid ice [*Huining et al.*, 1999; *Scott et al.*, 2006]. Signals at radar frequencies (Ku band ~13.6 GHz) will penetrate beyond the snow-air interface and backscatter from the upper parts of the snow strata [*Mätzler and Wegmüller*, 1987]. Such radar frequency signals cannot penetrate through solid ice.

Repeated radar altimetry measurements of ice sheet surface topography have been widely used to monitor recent changes [*Khvorostovsky*, 2012; *Zwally et al.*, 2011; *Li and Davis*, 2008; *Johannessen et al.*, 2005]. There are challenges associated with using radar data to estimate the volume change of the Greenland Ice Sheet (GrIS) because of the signal penetration into the snow, particularly the temporal and spatial changes of the penetration depth.

In July 2012, the GrIS underwent the most extensive melt event observed in recent time, with 98.6% of the surface experiencing melt on 12 July [*Nghiem et al.*, 2012]. Above-average surface temperatures were observed across the ice sheet during a period of 1 week, after which the temperature returned to normal conditions *Hall et al.* [2013].

We expect that the 2012 melt event had a significant impact on derived CryoSat-2 data over the interior part of the GrIS, as proposed by *Forsberg et al.* [2013]. We hypothesize that the event led to an abrupt change in surface scattering properties in the dry-snow zones due to the sudden formation of ice layers near the snow surface. The change in scattering properties seen from the Ku-frequency band would affect the inferred surface elevation of the ice sheet and possibly introduce a regional elevation bias. Such a bias could be

misinterpreted as an actual elevation change of the GrIS, as also theorized by *Scott et al.* [2006]. To investigate the effect of the melt event on surface height retrieval from radar altimetry, we analyze the CryoSat-2 level 2 intermediate (L2i) data product, provided by the European Space Agency (ESA), to determine whether an elevation bias was introduced into the product due to the 2012 melt event. Additionally, we undertake a detailed study of CryoSat-2 low-resolution mode (LRM) level 1b (L1b) data, and extract additional information about the shape of the radar waveforms than is available in the L2i product. This study focuses on an area around the North Greenland Eemian Ice Drilling Project (NEEM) (located at 77.45°N and 51.06°W, in northwest Greenland), where in situ data is available and used to validate and interpret the results derived from the processed CryoSat-2 L1b observations.

2. Data and Methods

CryoSat-2 operates both in the low-resolution mode (LRM) and the interferometric synthetic aperture mode (SARin) over the GrIS. We use several types of CryoSat-2 data sets to study the measurable effects on surface elevation changes at different spatial scales. Initially CryoSat-2 L2i data [*ACS Team and MSSL Team*, 2011] were used to assess ice sheet-wide elevation changes. A more detailed description of the use of the CryoSat-2 L2i data is given in the supporting information, however, in essence the CryoSat-2 L2i data provides the user with the position and the elevation of the radar return. To date, the ESA L2/L2i data contain little information on the shape of the waveforms (only two parameters describing the received backscattered power) which could be used to identify changes in scattering properties of the surface. Hence, to obtain a more detailed study of the effects of abnormal weather conditions on surface height estimation, we additionally processed and analyzed CryoSat-2 LRM L1b data at different spatial scales (locally ~25 km and regionally ~300 km) around the NEEM-camp. In this process we estimated surface height and additional waveform parameters. In addition to the backscatter and the peakiness (available in the ESA L2/L2i product), the leading edge width and trailing edge slope was estimated from the radar waveforms [*Legresy and Rémy*, 1997].

The backscatter (Bs) is controlled by the surface and volume echo and can be used to discriminate between different surface types (e.g., high backscatter would reveal a very smooth surface) [*Legresy and Rémy*, 1997]. The width of the leading edge waveform (LeW) is related to the microroughness of the small-scale topography and surface penetration effects of the radar signal [*Legresy and Rémy*, 1997]. A large leading edge width would be indicative of volume scattering of the signal in the upper parts of the firn, while a small leading edge would correspond to surface scattering. The trailing edge slope (TeS) of the waveform is mainly controlled by the ratio between volume and surface scattering, where a very high slope would reveal a very specular surface [*Legresy and Rémy*, 1997]. The peakiness (PP) of the waveform is a statistical measure of how specular the waveform is and can be used to discriminate between different surface types [*Laxon*, 1994]. The derivation and definition of these parameters can also be found in the supporting information.

In this study the LRM L1b data were retracked using a 20% threshold retracker constructed to track the first peak of the waveform. The choice of retracking point is based on the requirements of robust and repeatable elevations [*Davis*, 1997], intended to reduce spurious changes in elevation resulting from the retracking procedure. For a regional analysis, data were collected for the months of June and August 2012 within a $3^\circ \times 3^\circ$ box centered around the NEEM site. The area below 2000 m elevation was excluded, to ensure dry-snow surface conditions prior to the melt event. For a local analysis, we analyzed CryoSat-2 20 Hz data within a radius of 0.2° around the NEEM site for the period of January 2011 to December 2013. More information is available in the supporting information about the processing procedures and the error estimation.

The local and regional data were then compared to in situ observations, obtained from the NEEM site. In situ data include surface observations, weather data, and snow pit samples collected before, during, and after the melt event. More information is available in the supporting information about the in situ data collected at the NEEM site. The regional analysis was performed to derive more robust statistics, as the spatial data coverage is usually quite sparse on local scales (~20 km) and at monthly time intervals.

3. Results

Figure 1a shows the difference in surface elevation between the months of May–June and August–September 2012 based on the ESA CryoSat-2 L2i data set. The figure shows a clear positive surface increase in the dry-snow zone. In the coastal regions, a surface lowering indicative of ablation is observed. Based on

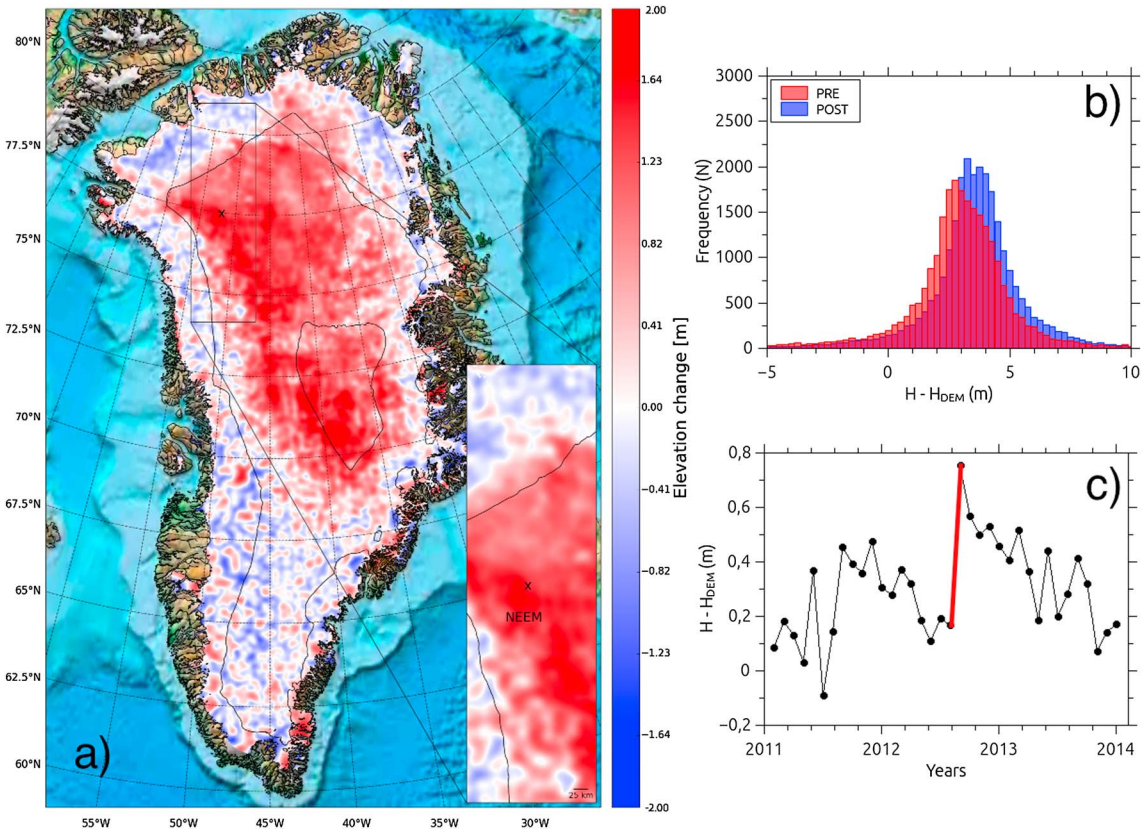

Figure 1. (a) Surface elevation differences between the May–June and August–September 2012 CryoSat-2 L2i data. The differences in surface elevation shows a clear positive increase in the dry-snow zone and ablation in the coastal regions. Black lines indicate the 2000 and 3000 m elevation contours. Found in the supporting information are 2011 and 2012 reference figures. (b, c) Histograms (regional analysis) and time series (local analysis) of the changes in surface elevation around NEEM estimated from the reanalyzed CryoSat-2 L1b data presented in this study. The 2012 elevation change is indicated in red.

the analysis of the L2i data set, we find that the magnitude of the positive surface elevation increase in the dry snow (above 2000 m and north of 70° latitude) is 89 ± 49 cm for the reported period, with an estimated surface elevation increase of 124 ± 51 cm at the NEEM site.

Analysis of the CryoSat-2 L1b data also shows an overall increase in surface elevation around NEEM, as a result of the 2012 melt event. The regional analysis of L1b data, retracked with the 20% threshold, shows an average surface height increase of 56 ± 26 cm (Figure 1b). This result agrees well with the local analysis of L1b data which shows a slightly lower average of 50±37 cm at NEEM. Figures 1b and 1c, respectively, shows a histogram and a time series of the detrended surface elevations for regional and local elevation changes. In Figure 1c a clear positive change in surface elevation (indicated in red) can be detected at the time of the melt event with a ∼42% larger magnitude than for the previous year. The surface elevation change persists for the duration of 2013 with a linear decrease in surface elevation.

Figure 2 shows histograms (regional) and time series (local) of the different waveform parameters for the months of June and August and the period 2011–2013, respectively. These histograms clearly indicate that there has been a major transition in all of the scattering properties considered here. We find that the backscattering coefficient (Bs) and pulse peakiness (PP) parameters have increased in magnitude over the melt event by 4.5% and 33%, respectively. Simultaneously, the leading edge width (LeW) and trailing edge slope (TeS) parameters decreased in magnitude by 55% and 29%, respectively. The most prominent change was observed in the PP and LeW parameters, which indicate that the surface has become more specular after the event. The increase in specularity is also followed by a prominent reduction in signal penetration depth and surface roughness, indicated by a decrease in the LeW parameter.

This pattern can also be detected in the standard deviation of the elevation difference in the satellite crossover points. Comparing the months of June and August, the standard deviation of the elevation difference of

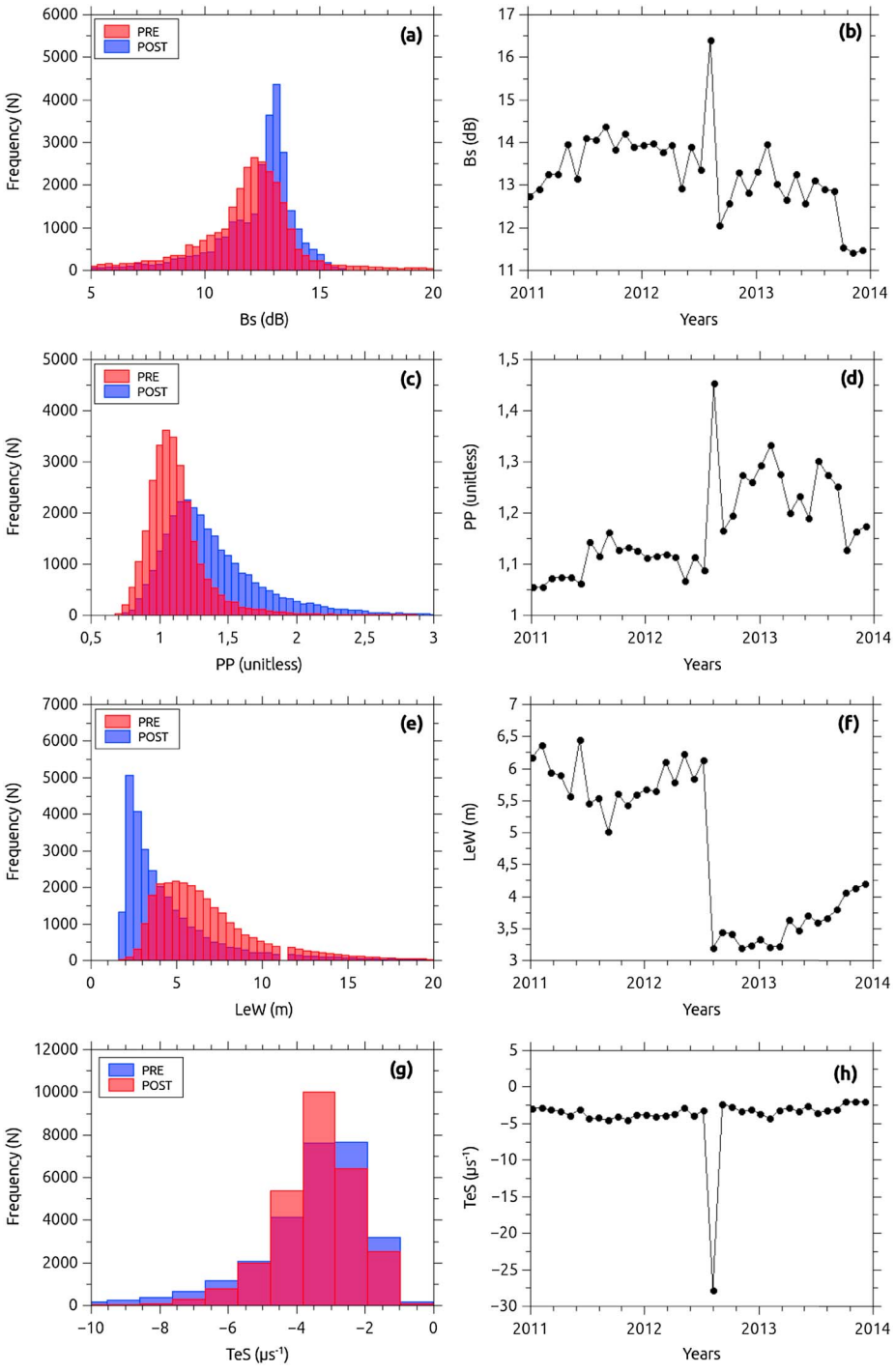

Figure 2. Histograms and time series, of waveform parameters (a,b) Bs, (c,d) PP, (e,f) LeW, and (g,h) TeS around NEEM site. The histograms depict the regional data between June and August 2012 and the time series the local data from 2011 to 2013.

the crossovers (June–August) was reduced from 26 to 18 cm, supporting the decrease in surface roughness indicated by the Bs and PP parameters.

Analyzing the time series in Figure 2, the 2012 melt event can clearly be detected from the sudden and striking waveforms parameter changes. Clear shifts can be detected in Figure 2 at the time of the melt event, connecting the change in scattering properties to the observed change in apparent elevation. These changes are most evident in the LeW and TeS parameters. The TeS parameter shows the largest change, as seen in Figure 2h,

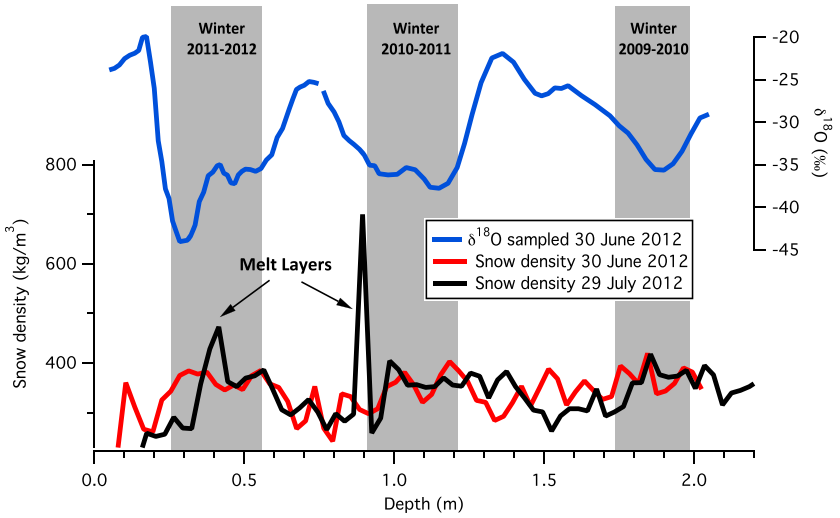

Figure 3. Density and oxygen isotope measurements from two snow pits sampled at NEEM site before and after the July 2012 melt event. The presence of ice layers after the melt event are clearly demonstrated by densities greater than 400 kg m^{-3}. Winter snow deposition layers were determined by oxygen isotope ratios and are indicated by gray bars. Note that the 29 July density profile depths have been corrected for the 13 cm lower postmelting surface.

with a change in magnitude of 85%. The change in TeS parameter is less observable in the June–August comparison histogram (Figure 2g), as the change is only observed in the month of July and then quickly recovers. After the melt event the Bs parameter decreases as the LeW parameter increases, indicating a buildup of a new snow cover at the NEEM site.

4. Validation Data

The NEEM site was occupied during the 2012 melt event, therefore, in situ observations are available to validate the CryoSat-2 data products evaluated here. The observations indicate that the elevation of the NEEM snow surface lowered between 11 and 18 July. The Greenland Climate Network (GC-NET) automatic weather station (AWS) [*Box and Rinke*, 2003] located at the NEEM site recorded daytime surface air temperatures above 0°C from 10 to 15 July, and rain was observed on 11 and 13 July. The surface snow was compacted as a result, with the AWS indicating a decrease in surface snow height of 13 ± 3 cm, based on the difference in mean snow surface levels from 5–10 to 18–23 July. The AWS data are confirmed by in situ observations of snow surfaces having lowered by 10 to 15 cm around camp structures. It is inferred that the snow beneath the camp structures was not significantly compacted because they were not directly exposed to sunlight, rain, and surface air temperatures.

A series of snow pits were sampled at NEEM between 30 June and 29 July, documenting the extensive warming of the topmost 60 cm of the snow and the formation of several solid ice layers. Daily snow temperature measurements indicate that the upper 20 to 60 cm of the NEEM snowpack was at or near the melting point (−0.3 ± 0.5°C) between 12 and 16 July. The formation of ice layers as a result of the warming is evident in Figure 3, where snow density is shown for snow pits sampled before and after the melt event. Premelt oxygen isotope ratios $\delta^{18}O$ measured in a snow pit (Figure 3) indicate summer and winter deposition strata [*Kuramoto et al.*, 2011]. The snow pit sampled on 30 June shows snow densities consistently less than 400 kg m^{-3} with higher densities corresponding to winter snow and lower densities corresponding to summer snow.

In contrast, the postmelting snow pit (29 July) shows the formation of a thin ice layer at 29 cm depth and a thick ice layer at 76.5 cm depth below the postmelt snow surface. We note that the summer/winter density variations are retained in the postmelting snow pit, despite the occurrence of physical processes such as surface compaction, water percolation, and ice layer formation. Several snow pits were sampled after the melt event, with ice layers usually present between 10–30 cm and 50–70 cm depth. These observations are in agreement with earlier reports from the site [*Nghiem et al.*, 2012] where ice layers were reported to have formed at approximately 5, 20, and 69 cm depth.

The surface observations presented here can be compared to theoretical calculations of the CryoSat-2 signal penetration depth to investigate the magnitude of possible elevation bias due to ice layer formation. Dielectric signal penetration models estimate the penetration depth of a Ku band radar into the dry-snow zone, based on various assumptions for snow density, temperature, impurity content, imaginary permittivity, and signal frequency. *Stiles and Ulaby* [1980] determined a signal penetration depth of approximately 100 cm in dry snow, with an order-of-magnitude reduction of penetration depth in wet snow or ice. The snow pit observations available from the NEEM site confirms the assumption of dry-snow conditions prior to the melt event. Hence, the theoretical penetration depth should be valid for the premelt snow surface. From Figure 3, it can be seen that the penetration depth calculated for dry snow includes summer and winter snow strata from calendar years 2012 and 2011. In addition to recrystallization of the snow pack following the melt event, the relatively dense (>500 kg m^{-3}) ice layers likely represent a strong dielectric discontinuity and therefore enhance the reflection of the Ku band energy. Considering the observed lowering of 13 ± 3 cm of the physical surface and the formation of ice layers postmelt, we suggest the two ice layers to acts as internal reflectors. The measured depths of these ice layers suggest the penetration depth further decreased by 27 ± 10 cm or 47 ± 10 cm, counting from the approximately 100 cm penetration depth of the premelt snow pack penetration depth. This positive change in penetration depth led to the apparent surface elevation increase observed in the CryoSat-2 data product.

5. Discussion

The rapid change in the surface conditions of the interior parts of the GrIS during the 2012 melt event manifests itself as an apparent and sudden increase in surface elevation, which can be observed by CryoSat-2 Ku band radar. The magnitude of this elevation bias is found to be 89 ± 49 cm when analyzing L2i elevation data, which is reduced to 56 ± 26 cm when analyzing the regional data derived from the L1b product around the area of NEEM. The apparent surface elevation increase can be clearly detected in the rapid elevation change in the region around NEEM, as seen in Figure 1. In Figure 1, both the histogram and time series of the parameters show the introduction of a positive elevation bias in the retracked L1b data. An elevation change of 56 cm would, according to *Thomas et al.* [2008], correspond to a 336 Gt increase in mass of the GrIS in the areas above 2000 m elevation, if it is assumed to be caused by snowfall. Such large positive mass changes in a high melt year are unlikely.

The waveform parameters considered here, shown in Figure 2, indicate that the elevation bias associated with the 2012 melt event has been introduced by a transition in scattering properties of the radar signal. In the dry-snow zone of the GrIS, the melt event has changed the scattering regime from volume toward surface scattering, which can be explained by the formation of a strong internal reflective layer in the form of ice lenses within the upper most snowpack. The occurrence of such a surface change was confirmed by in situ observations at NEEM (Figure 3). The changed snow conditions at NEEM suggest an increase in altitude of the radar reflector to the ice layer closest to the physical surface. From a dry-snow penetration depth of 100 cm, the formation of ice layers produced an increase in penetration depth of 47 ± 10 cm, which is in good agreement with the CryoSat-2 results. The transition from volume to surface scattering is especially apparent in the LeW waveform parameter, where a dramatic reduction in the width of the leading edge is observed at the time of the melt event. This reduction of the width of the leading edge is indicative of a decrease in the magnitude of the surface penetration of the signal, i.e., a reduction in volume scattering.

The time series of the waveform parameters in Figure 2 show a clear signal at the time of the melt event. The behavior and duration of each parameter varies, depending upon the underlying physics governing the behavior of each parameter. The Bs, PP, and TeS parameters are especially sensitive to the specularity of the surface. Therefore, abrupt spikes in these parameters would be expected when the surface becomes wet and the smoothness of the surface increases. This behavior is also observed in the Bs, PP, and TeS parameters, as seen in Figures 2b, 2d, and 2h, at the time of the melt event. These signals are expected to be short lived as the centimeter-scale surface roughness will increase when the surface refreezes, thereby reducing the scattered power. The LeW (Figures 2e and 2f) parameter, however, should be more long lived, as it is more dependent upon surface penetration effects.

It is found that the melt event signal in the LeW parameter is more persistent and longer lasting than for the other three parameters considered here. As shown in Figure 2f, the LeW parameter shows a distinct decrease at the time of the event and can be seen to increase linearly as new snow is deposited on the surface.

This behavior is also observed in the Bs parameter, where a linear decrease occurs after the melt event. The anticorrelation between LeW and Bs parameters is expected as the surface roughness and surface penetration will increase with new snow deposition. The behaviors of these parameters increases our confidence in the measurement of real and physical signals in our waveform parameters. However, from the Bs, PP, and TeS parameters alone it is not clear if the melt event signal is short or long lived. The LeW-parameter on the other hand provides support for the notion that the melt-related elevation bias is more long lived. The reflective ice layer caused by the melt event would continue to be the dominant scattering surface until enough snow has been deposited to bury the ice layer below the maximum penetration depth of the signal. This is also what we observe in the time series of the elevation change in Figure 1c, where at the time of the melt event the magnitude of the elevation change signal increases twofold (indicated by red line) and persists for a duration of approximately 1 year.

Future derivations of surface elevation changes needs to account for the changes induced by changes in the surface snow scattering parameters explored here. The ESA CryoSat-2 L2/L2i product does not currently include sufficient information to undertake such efforts, as it includes limited information regarding the waveform. Furthermore, it is unclear that the inclusion of these parameters in the estimation procedure would give the desired effects, as the melt event caused a stepwise change in elevation persisting for $\sim$1 year. The stepwise nature and the temporal evolution of the depth of the ice layer could possibly limit the effectiveness of the method of *Flament and Rémy* [2012], who proposed a least squares model to parametrize the correlations between elevation changes and waveform parameters. Another possible approach could be to apply a bias-correcting scheme, based on the elevation change data presented her, but it should be noted that the magnitude of the bias is spatially variable and retracker dependent.

The retracker dependence is clearly evident when analyzing the L2i and L1b data, where the height bias at NEEM approximately 60% between the two data sets. The use of different retracking thresholds can easily introduce variations of 70 cm, as observed in this study in the process of determining the optimal retracking threshold. Understanding the retracker and its applied retracking correction is important when trying to account for the effects of melt events. The melt event provides an interesting opportunity to investigate retracker-dependent surface penetration on a continental scale. This has previously only been possible by using airborne laser data or other noncontemporary satellite missions, such as ICESat, for validation of the results.

Quantifying melt-related biases in radar altimetric data is important for determining the reliability of CryoSat-2 data products. From this case study around NEEM, we suggest that the LeW and TeS parameters could be used to detect melt events in radar altimetry data, as they show the largest changes of the waveform parameters (see Figures 2f and 2h). The TeS parameter is here of particular interest because it can be used to detect melt events near the surface, giving a very precise timing of the event. This is because wet snow surface is very specular, which makes the trailing edge slope (TeS) extremely sharp. Once the refreezing process has begun the surface roughness will increase and thus the absolute magnitude of the TeS signal will be lowered, as seen in Figure 2h.

Even though the melt event is a transient signal it has the possibility to affect longer-term elevation change trends in the dry-snow zone above 2000 m. This is due to the long-lived domination of the near-surface ice layer created by the melt event, which should therefore be considered when determining elevation change trends based on radar altimetry spanning this period of 2012–2013. Our immediate recommendations for the use of the CryoSat-2 L2 product, for now, is to flag measurements subject to abnormal melt conditions such as the 2012 melt event and wait for dry-snow conditions to reoccur. This challenges the real-time application of radar altimetry to study elevation changes of ice sheets in a warming climate, especially in locations in Greenland and Antarctica where dry-snow conditions currently occur.

6. Conclusion

The 2012 melt event introduced a significant ice sheet-wide elevation bias over the GrIS dry-snow zone (Figure 1a). In the proximity of the NEEM site the elevation change bias was found to be 56 ± 26 cm, obtained from a detailed analysis of processed CryoSat-2 L1b data presented in this study. This is in contrast to the ESA L2i derived elevation change bias, which was found to be 89 ± 49 cm for the same area.

Theoretical modeling of radar penetration depth in conjunction with in situ measurements were able to attribute the bias to changes in radar scattering waveform parameters. The bias was caused by the introduction of ice layers in the upper most snowpack. The ice layers act as strong reflectors for the radar signal emitted by CryoSat-2 and transformed the scattering regime from volume to near-surface scattering. Detailed analysis of the waveform parameters confirms this interpretation, with an abrupt change in the magnitude of all four waveform parameters occurring at the time of the 2012 melt event.

The estimated magnitude of the elevation change bias also showed a clear dependence upon the applied retracker correction. Therefore, information about the applied retracking correction is important when trying to account for elevation biases induced by melt events, as the size of the correction has a direct effect on the magnitude of the elevation bias. The 2012 melt event provided a unique opportunity to study CryoSat-2 radar penetration depth in the interior part of the Greenland ice sheet and evaluate retracker dependencies in relation to altimetry-derived mass balance studies.

Acknowledgments

This publication is contribution number 47 of the Nordic Centre of Excellence SVALI, Stability and Variations of Arctic Land Ice, funded by the Nordic Top-level Research Initiative (TRI). NEEM is directed and organized by the Center of Ice and Climate at the Niels Bohr Institute and U.S. NSF, Office of Polar Programs. It is supported by funding agencies and institutions in Belgium (FNRS-CFB and FWO), Canada (NRCan/GSC), China (CAS), Denmark (FIST), France (IPEV, CNRS/INSU, CEA, and ANR), Germany (AWI), Iceland (RannIs), Japan (NIPR), Korea (KOPRI), The Netherlands (NWO/ALW), Sweden (VR), Switzerland (SNF), United Kingdom (NERC), and the USA (U.S. NSF, Office of Polar Programs). CryoSat-2 L1b and L2i data are available from the European Space Agency via download at (www.earth.esa.int). NEEM snow pit data are available from (http://www.iceandclimate.nbi.ku.dk/data). The authors thank two anonymous reviewers for their constructive comments.

The Editor thanks two anonymous reviewers for their assistance in evaluating this paper.

References

ACS Team, and MSSL Team (2011), *CRYOSAT Ground Segment, Instrument Processing Facility l2, l2 Products Format Specification*, European Space Agency. CS-RS-ACS-GS-5123.

Box, J. E., and A. Rinke (2003), Evaluation of Greenland Ice Sheet surface climate in the HIRHAM regional climate model using automatic weather station data, *J. Clim.*, *16*, 1302–1319, doi:10.1175/1520-0442-16.9.1302.

Davis, C. H. (1997), A robust threshold retracking algorithm for measuring ice-sheet surface elevation change from satellite radar altimeters, *IEEE Trans. Geosci. Remote Sens.*, *35*(4), 974–979, doi:10.1109/36.602540.

Flament, T., and F. Rêmy (2012), Dynamic thinning of Antarctic glaciers from along-track repeat radar altimetry, *J. Glaciol.*, *58*(211), 830–840, doi:10.3189/2012JoG11J118.

Forsberg, R., L. Sørensen, J. Levinsen, and J. Nilsson (2013), Mass loss of Greenland from GRACE, ICESat and CryoSat, in *Proceedings of the CryoSat Workshop, Dresden, ESA Special Publication 717, Paper S6-4*.

Hall, D. K., J. C. Comiso, N. E. DiGirolamo, C. A. Shuman, J. E. Box, and L. S. Koenig (2013), Variability in the surface temperature and melt extent of the Greenland ice sheet from MODIS, *Geophys. Res. Lett.*, *40*, 2114–2120, doi:10.1002/grl.50240.

Huining, W., J. Pulliainen, and M. Hallikainen (1999), Effective permittivity of dry snow in the 18 to 90 GHz range, *Prog. Electromagn. Res.*, *24*, 119–138, doi:10.1163/156939399X00727.

Johannessen, O. M., K. Khvorostovsky, M. W. Miles, and L. P. Bobylev (2005), Recent ice-sheet growth in the interior of Greenland, *Science*, *310*(5750), 1013–1016, doi:10.1126/science.1115356.

Khvorostovsky, K. S. (2012), Merging and analysis of elevation time series over Greenland Ice Sheet from satellite radar altimetry, *IEEE Trans. Geosci. Remote Sens.*, *50*(1), 23–36, doi:10.1109/TGRS.2011.2160071.

Kuramoto, T., K. Goto-Azuma, M. Hirabayashi, T. Miyake, H. Motoyama, D. Dahl-Jensen, and J. P. Steffensen (2011), Seasonal variations of snow chemistry at NEEM, Greenland, *Ann. Glaciol.*, *52*(58), 193–200, doi:10.3189/172756411797252365.

Laxon, S. (1994), Sea ice altimeter processing scheme at the EODC, *Int. J. Remote Sens.*, *15*(4), 915–924, doi:10.1080/01431169408954124.

Legresy, B. L., and F. Rêmy (1997), Altimetric observations of surface characteristics of the Antarctic Ice Sheet, *J. Glaciol.*, *43*(144), 265–275.

Li, Y., and C. H. Davis (2008), Decadal mass balance of the Greenland and Antarctic Ice Sheets from high resolution elevation change analysis of ERS-2 and Envisat radar altimetry measurements, in *IEEE International Geoscience and Remote Sensing Symposium, IGARSS 2008*, vol. 4, pp. IV–339–IV-342, IEEE, Boston, Mass.

Mätzler, C., and U. Wegmüller (1987), Dielectric properties of fresh-water ice at microwave frequencies, *Phys. D: Appl. Phys.*, *20*, 1623–1630, doi:10.1088/0022-3727/20/12/013.

Nghiem, S. V., D. K. Hall, T. L. Mote, M. Tedesco, M. R. Albert, K. Keegan, C. A. Shuman, N. E. DiGirolamo, and G. Neumann (2012), The extreme melt across the Greenland Ice Sheet in 2012, *J. Glaciol.*, *54*(185), 203–212, doi:10.1029/2012GL053611.

Scott, J. B. T., P. Nienow, D. Mair, V. Parry, E. Morris, and D. J. Wingham (2006), Importance of seasonal and annual layers in controlling backscatter to radar altimeters across the percolation zone of an ice sheet, *Geophys. Res. Lett.*, *33*, L24502, doi:10.1029/GL027974.

Stiles, W. H., and F. T. Ulaby (1980), Dielectric properties of snow, *NASA contract, Tech. Rep. CR 166764*, Kans. Univ. Cent. for Res., Inc.; Remote Sensing Lab., Lawrence.

Thomas, R., C. Davis, E. Frederick, W. B. Krabill, Y. Li, S. Manizade, and C. Martin (2008), A comparison of Greenland Ice-Sheet volume changes derived from altimetry measurements, *Geophys. Res. Lett.*, *39*, L20502, doi:10.3189/002214308784886225.

Zwally, H., et al. (2011), Greenland Ice Sheet mass balance: Distribution of increased mass loss with climate warming 2003–2007 versus 1992–2002, *J. Glaciol.*, *58*(201), 88–102, doi:10.3189/002214311795306682.